Supplemental Material for

# Design requirements for interfering particles to maintain co-evolutionary stability with HIV-1

Igor M. Rouzine and Leor S. Weinberger

**Table of Contents**

**Introductory note on terminology for models**

Throughout this supplementary information section (and the main text) we refer to two scales of models: (i) the intracellular model which is at the scale of a single infected cell, and (ii) the *in vivo* model which refers to the scale of the individual infected person or "host". Though "*in vivo*" can refer to cells in a tissue-culture setting (especially in the field of biochemistry), in an attempt to minimize confusion we follow the usage in the virology and HIV fields which use *in vivo* to refer exclusively to the level of the whole organism (i.e. within patients or non-human primates).

## A. Capsid stealing model

*Basic equations and biological interpretation*

Consider a cell with an integrated HIV provirus. Of all virus products, we focus on two: $C(t)$, the amount of fully formed capsids that do not yet carry genomic mRNA dimers, and $G(t)$, the amount of dimers of genomic mRNA. The system of equations has the form

$$\frac{dG}{dt} = \underbrace{\theta}_{\substack{\text{HIV genome}\\ \text{production}}} - \underbrace{k_{pck}GC}_{\substack{\text{Packaging of}\\ \text{HIV genomes}\\ \text{into capsids}}} - \underbrace{\alpha G}_{\substack{\text{Loss of}\\ \text{HIV genomes}}} \qquad (1)$$

$$\frac{dC}{dt} = \underbrace{\eta\theta}_{\substack{\text{Capsid}\\ \text{production}}} - k_{pck}GC - \underbrace{\beta C}_{\substack{\text{Loss of}\\ \text{capsids}}} \qquad (2)$$

Model parameters are: $\theta$, the linear production rate of HIV genomes; $k_{\text{pck}}$, packaging efficiency; $\alpha$ and $\beta$, the exponential rates of genome and capsid loss, respectively; and, $\eta$, the capsid-to-genome production ratio (see Table S1).

In a cell infected with HIV provirus and co-infected with $m$ copies of a (DIP) provirus, the system of equations (as given in the main text in Eqs. 1-3) has the form:

$$\frac{dG}{dt} = \underbrace{\theta}_{\substack{\text{HIV genome}\\ \text{production}}} - \underbrace{k_{\text{pck}}GC}_{\substack{\text{Packaging of}\\ \text{HIV genomes}\\ \text{into capsids}}} - \underbrace{\alpha G}_{\substack{\text{Loss of}\\ \text{HIV genomes}}} \qquad (3)$$

$$\frac{dC}{dt} = \underbrace{\eta\theta}_{\substack{\text{Capsid}\\ \text{production}}} - k_{\text{pck}}(G + G_{\text{DIP}})C - \underbrace{\beta C}_{\substack{\text{Loss of}\\ \text{capsids}}} \qquad (4)$$

$$\frac{dG_{\text{DIP}}}{dt} = \underbrace{mP\theta}_{\substack{\text{DIP genome}\\ \text{production}}} - \underbrace{k_{\text{pck}}G_{\text{DIP}}C}_{\substack{\text{Packaging of}\\ \text{DIP genomes}\\ \text{into capsids}}} - \underbrace{\alpha G_{\text{DIP}}}_{\substack{\text{Loss of}\\ \text{DIP genomes}}} \qquad (5)$$

where $G_{\text{DIP}}(t)$ is concentration of DIP genomes, and parameter $P$ is the ratio of DIP to HIV genome production rates. As previously demonstrated [1,2], $P > 1$ is required for a therapeutic effect so $P > 1$ is used. Multiplicity of DIP infection $m$ is any integer number, $m$=1, 2, 3, … .

The packaging coefficients for HIV and DIP are assumed to be the same ($k_{\text{pck}}$). Indeed, mutation in the packaging domain of HIV *gag* equally affects packaging of particles that share the same

stem loop 3 (SL3) sequence. Below, we study evolution of HIV affecting $k_{pck}$. (A double mutation in HIV, one in *gag* decreasing $k_{pck}$ and another in HIV-1 stem-loop 3—SL3, the so-called Ψ region—compensating for this effect, could decrease $k_{pck}$ for DIP but not for HIV. However, the same compensatory mutation will occur in DIP SL3, only much more quickly, because it is a single mutation. Therefore equality of the two packaging constants will be preserved.)

Below we will consider a dually infected cell (containing an integrated HIV provirus and $m$ copies of integrated DIP provirus) because a singly infected cell can be considered a particular case of a dually infected cell with $P = 0$ or $m = 0$.

*Stead-state calculations*

Here, we assume that sufficient time has passed after infection of a cell so that steady state has been reached. For dually infected cells (Eqs. 3–5), steady-state amounts of genomes and capsids are given by the equations:

$$G = \frac{\theta}{\alpha + k_{pck} C} \tag{6}$$

$$C = \frac{\eta\theta}{\beta + k_{pck}(G + G_{DIP})} \tag{7}$$

$$G_{DIP} = \frac{mP\theta}{\alpha + k_{pck} C} \tag{8}$$

It is convenient to introduce a rescaled capsid number $y$ defined as

$$y = k_{pck} C / \alpha \tag{9}$$

In this notation, Eqs. 6–8 are equivalent to

$$G = \frac{\theta}{\alpha(1+y)} \tag{10}$$

$$G_{DIP} = \frac{mP\theta}{\alpha(1+y)} \tag{11}$$

where

$$\kappa y^2 + (mP + 1 - \eta + \kappa) y - \eta = 0 \tag{12}$$

and

$$\kappa = \frac{\alpha\beta}{\theta k_{pck}} \tag{13}$$

Here, $\kappa$ is the composite "waste parameter" contrasting the loss of HIV genomes and capsids against genome production and packaging. The solution of Eq. 12 has the form

$$y = \frac{1}{2\kappa}\left[-\left(mP + 1 - \eta + \kappa\right) + \sqrt{\left(mP + 1 - \eta + \kappa\right)^2 + 4\eta\kappa}\right] \quad (14)$$

*Burst sizes of HIV and DIP and connection to the in vivo level*

To connect to HIV and DIP dynamics at the level of an individual host, we need to predict the burst size (total number of particles produced per cell lifetime) of HIV in singly (HIV+DIP-) and dually (HIV+DIP+) infected cells, and that of DIP in dually infected cells. Based on previous analysis [1], we assume that steady-state viral production is reached shortly after the cell is infected and long before the death of the infected cell. Then, the total numbers of virus particles per cell are given by

$$n = k_{\mathrm{pck}}\left[GC\right]_{P=0} / \delta \quad (15)$$

$$\psi_m n = k_{\mathrm{pck}} GC / \delta \quad (16)$$

$$\rho_m \psi_m n = k_{\mathrm{pck}} G_{\mathrm{DIP}} C / \delta \quad (17)$$

Here, $n$ is the HIV burst size from a cell infected with HIV only (the case obtained by setting $P = 0$), $\psi_m$ shows decrease in HIV burst size due to co-infection with DIP, $\rho_m$ is the ratio of DIP to HIV burst size in a co-infected cell, and $1/\delta$ is the average lifetime of an HIV-infected cell.

Substituting Eqs. 9–11 for steady-state values of $G$, $G_{\mathrm{DIP}}$, and $C$ into Eqs. 15–17, we arrive at

$$n = \frac{\theta}{\delta}\frac{y}{1+y}\bigg|_{P=0} \quad (18)$$

$$\psi_m n = \frac{\theta}{\delta}\frac{y}{1+y} \quad (19)$$

$$\rho_m = \frac{G_{\mathrm{DIP}}}{\mathrm{G}} = mP \quad (20)$$

Here, the rescaled capsid concentration, $y$, is given by Eq. 14 and the multiplicity of infection, $m$, runs from 1 to infinity.

*Case of small waste parameter $\kappa << 1$*

As we show in Section C below, HIV evolution is directed towards decrease of the waste parameter. Therefore, the case of small $\kappa$ is of considerable practical interest. When $\kappa << 1$, Eq. 14 for $y$ can be approximated by a simpler expression depending on sign of $mP + 1 - \eta$, as given by

$$y = \begin{cases} \dfrac{\eta}{1+mP-\eta} & \eta < mP+1 \quad (21) \\ \dfrac{\eta-1-mP}{\kappa} & \eta > mP+1 \quad (22) \end{cases}$$

Substituting $y$ from Eqs. 21 and 22 into Eqs. 18 and 19, and evaluating them in the limit $\kappa \to 0$, we obtain

$$n = \begin{cases} \theta/\delta, & \eta > 1 \\ \eta\theta/\delta & \eta < 1 \end{cases} \quad (23)$$

and

$$\psi_m n = \begin{cases} \dfrac{\theta}{\delta} & \eta > 1+mP \\ \dfrac{\theta}{\delta}\dfrac{\eta}{1+mP} & \eta < 1+mP \end{cases} \quad (24)$$

respectively. Combining Eqs. 23 and 24, for the value of the HIV suppression factor in dually infected cells $\psi_{\mathrm{m}}$ we obtain

$$\psi_m = \begin{cases} \dfrac{1}{1+mP} & \eta < 1 \quad (25) \\ \dfrac{\eta}{1+mP} & 1 < \eta < 1+mP \quad (26) \\ 1 & \eta > 1+mP \quad (27) \end{cases}$$

## B. HIV and DIP load at the level of an individual host

*Basic equations and biological interpretation*

We begin with the well-parameterized "standard" model of HIV-virus *in vivo* dynamics [3,4] and, similar to the method we have previously used [1,2], we generalize this model to include production of DIP particles. The generalized model includes co-infection of cells with DIP and HIV, so that dually infected cells produce less HIV. In comparison to the previous versions [1,2], we relax the restriction of one copy of DIP provirus per cell. Based on results of recent *in vivo* studies [5], we postulate a single HIV provirus per cell.

The system of equations has the form:

$$\frac{dT}{dt} = b - \left(d + kV + kV_{\mathrm{DIP}}\right)T \tag{28}$$

$$\frac{dI}{dt} = kVT - \delta I \tag{29}$$

$$\frac{dT_{\mathrm{DIP}\,m}}{dt} = kV_{\mathrm{DIP}}T_{\mathrm{IP}\,m\text{-}1} - \left(d + kV + kV_{\mathrm{DIP}}\right)T_{\mathrm{DIP}\,m},\ m = 1,2,3,\ldots \tag{30}$$

$$\frac{dI_{\mathrm{D}\,m}}{dt} = kVT_{\mathrm{DIP}\,m} - \delta I_{\mathrm{D}\,m},\ m = 1,2,3,\ldots \tag{31}$$

$$\frac{dV}{dt} = n\delta I + n\delta\sum_{m=1}^{\infty}\psi_m I_{\mathrm{D}\,m} - cV \tag{32}$$

$$\frac{dV_{\mathrm{DIP}}}{dt} = n\delta\sum_{m=1}^{\infty}\rho_m\psi_m I_{\mathrm{D}\,m} - cV_{\mathrm{DIP}} \tag{33}$$

Here, the state variables are (as described in Table S2): $T$, uninfected CD4 T cells permissive for viral replication; $I$, cells infected with HIV only; $T_{\mathrm{DIP}\,m}$, CD4 T cells harboring $m$ copies of DIP provirus but not infected with HIV (by definition, $T_{\mathrm{DIP}\,0} = T$); $I_{\mathrm{D}\,m}$, "dually infected" cells harboring a copy of HIV and $m$ copies of DIP provirus; $V$, HIV load (free virus concentration in peripheral blood plasma); $V_{\mathrm{DIP}}$, DIP load.

The model parameters, which are well described in the literature, are: $b$, linear production rate of uninfected cells; $d$, natural death rate of uninfected cells; $k$, infectivity factor; $\delta$, death rate of singly and dually infected cells; $n$, HIV burst size from a singly infected cell. There are two additional parameters in the presence of DIP: $n\psi_{\mathrm{m}}$, HIV burst size from a dually infected cell with $m$ copies of DIP provirus; and $n\rho_m\psi_{\mathrm{m}}$, DIP burst size from a dually infected cell with $m$ copies of DIP provirus. These parameters are summarized in Table S2.

The biological interpretation of Eqs. 28–33 is that uninfected cells that are permissive for viral replication ($T$) are replenished from a constant source and depleted by three competing processes: (i) their natural death, (ii) infection by HIV particles, (iii) or infection by IPs (Eq. 28). Cells that become infected by HIV ($I$) produce viral particles and die at average rate $\delta \sim 1/$ day (Eq. 29). Alternatively, before becoming infected with HIV, a cell can be infected with one or more copies of DIP provirus ($T_{\mathrm{IP}}$) and we classify these cells according to the copy number of DIP proviruses by cell 'bins' $T_{\mathrm{IP}\,1}$, $T_{\mathrm{IP}\,2}$, $T_{\mathrm{IP}\,3}$, …, $T_{\mathrm{IP}\,m}$, … (Eq. 30). Cells infected with DIP alone do not express HIV proteins and die at the same rate as uninfected cells. If a $T_{\mathrm{IP}}$ cell is subsequently infected with HIV, the cell becomes "dually infected" ($I_{\mathrm{D}\,m}$,) and begins producing both HIV and DIP particles (Eq. 31). These dually infected cells ($I_{\mathrm{D}\,m}$) are $\mathrm{HIV}^{+}\mathrm{DIP}^{+}$ and die as rapidly as singly infected cells, $I$, which are $\mathrm{HIV}^{+}\mathrm{DIP}^{-}$. Thus, HIV particles are generated from both singly and dually HIV-infected cells (Eq. 32).

*Steady-state calculations*

Chronic HIV infection represents an approximate steady state. Setting the right-hand side (RHS) of Eqs. 28-33 to zero, we obtain

$$T = \frac{b}{d(1+v+v_{\mathrm{DIP}})} \tag{34}$$

$$I = \frac{kVT}{\delta} = \frac{b}{\delta(1+v+v_{\mathrm{DIP}})} \tag{35}$$

$$T_{\mathrm{DIP}\,m} = Tq^m \tag{36}$$

$$I_{\mathrm{D}m} = Iq^m \tag{37}$$

$$1+v+v_{\mathrm{DIP}} = R_0\left(1+\sum_{m=1}^{\infty}\psi_m q^m\right) \quad \text{or } v=0 \tag{38}$$

$$\left(1+v+v_{\mathrm{DIP}}\right)^2 = R_0 v\sum_{m=1}^{\infty}\rho_m\psi_m q^m \quad \text{or } v_{\mathrm{DIP}}=0 \tag{39}$$

where, for tractability, the following new notation is used:

$$R_0 = \frac{nkb}{cd} \tag{40}$$

$$v = \frac{kV}{d}, \quad v_{\mathrm{DIP}} = \frac{kV_{\mathrm{DIP}}}{d} \tag{41}$$

$$q = \frac{V_{\mathrm{DIP}}}{d+kV+kV_{\mathrm{DIP}}} = \frac{v_{\mathrm{DIP}}}{1+v+v_{\mathrm{DIP}}} \tag{42}$$

Here, $R_0$ is the basic reproduction ratio in the beginning of infection, $v$ and $v_{\mathrm{DIP}}$ are rescaled HIV and DIP loads. New notation $q$ determines the average number of integrated DIP provirus copies $E[m]$ in a dually infected cell, as given by

$$E[m] = \frac{\sum_{m=1}^{\infty} mq^m}{\sum_{m=1}^{\infty} q^m} = \frac{q\frac{d}{dq}\sum_{m=1}^{\infty} q^m}{\sum_{m=1}^{\infty} q^m} = \frac{1}{1-q} \tag{43}$$

HIV load ($v$) and DIP load ($v_{\mathrm{DIP}}$) in Eqs. 34–39 can be obtained by solving Eqs. 38 and 39 together with respect to $v$ and $v_{\mathrm{DIP}}$. Note that $q$ entering these equations depends on $v$ and $v_{\mathrm{DIP}}$ as given by Eq. 42 and must be calculated to be self-consistent.

*Calculation for Fig 2: HIV load is stably decreased by the presence of DIP*

MATLAB™ (version R2011a) was used to perform the calculation of $q$, $v$ and $v_{\mathrm{DIP}}$ through numerical iteration (although in certain important cases, such as the case of small $\kappa$ and large $P$, this calculation can be performed analytically, with asymptotic accuracy). The two parameters of the *in vivo* model reflecting the effect of DIP, $\rho_m$ and $\psi_m$, can be expressed in terms of intracellular parameters $\kappa$, $\eta$, and $mP$, as given by Eqs. 14 and 18–20. Therefore, the total rescaled HIV load and the total DIP load, as well as other important properties of the steady state

in an individual, depend on four dimensionless parameters: $R_0$, $P$, $\kappa$, and $\eta$. Results for HIV and DIP loads as functions of $\kappa$ and $P$ at different $\eta$ are shown in Fig. 2.

We observe that HIV is stably suppressed by DIP in a broad parameter range (Fig. 2b,d). One reason is that multiple infection of cells by DIP amplifies its effect on HIV. The average multiplicity of DIP infection, E[$m$] =1/(1-$q$), is rather large even at modest values of $\eta$ and $P$ (see Fig. S3a, below). Indeed, restricting DIP MOI to one, as previously assumed in ref. [1], considerably limits the degree and the parameter range of DIP interference (see Fig. S3b). In agreement with previous findings [1], the degree of HIV suppression and DIP load are rather sensitive to the DIP-to-HIV expression asymmetry, $P$ (Fig. 2d,e).

The decrease in HIV load, as compared to its value at $\kappa = 0$, $R_0 = 10$, is only partly due to the presence of DIP. The remainder of the decrease is due to increased waste, $\kappa$, which decreases the HIV burst size $n$ (Eqs. 14 and 18). We factored in this increased-waste effect by changing the value of $R_0$ proportionally. For reference, HIV load at zero DIP load (i.e., at $P = 0$) is shown in Fig. 2b as black dotted lines. The contribution of DIP to the decrease of HIV load at each given $\kappa$ is also shown (Fig. S2).

*Dynamic stability of DIP in vivo*

In principle, it is important to determine the parameter range in which the HIV-1 steady state with DIP is stable. However, because we are ultimately interested in analyzing whether DIP can autonomously spread between HIV-infected individuals as in [1], we use a more stringent criterion: we analyze whether DIP-free states are unstable (i.e., whether a small amount of DIP added to an DIP-free steady-state virus population will expand and result in a new steady state, where both HIV and DIP are present). We start from the DIP-free state ($V_{\mathrm{DIP}} = I_{\mathrm{D}m} = T_{\mathrm{DIP}m} = 0$) and Eqs. 34–39 reduce to a well-known result (for reviews, see refs. [3,4])

$$T = \frac{b}{dR_0}$$
$$V = \frac{d\left(R_0 - 1\right)}{k} \qquad (44)$$
$$I = \frac{b\left(R_0 - 1\right)}{\delta R_0}$$

At time $t = 0$, we introduce a small amount of DIP, $V_{\mathrm{DIP}}(0)$, and determine whether $V_{\mathrm{DIP}}(t)$, $I_{\mathrm{D}m}(t)$, and $T_{\mathrm{DIP}m}(t)$ will expand or contract in time. We do not need to solve dynamics of the entire set of Eqs. 28–33 because DIP load is initially low and DIP-infected cells are initially few such that HIV-related variables $T$, $V$, and $I$ are weakly perturbed and can be approximated with their previous respective steady-state levels. Hence, $V_{\mathrm{DIP}}(t)$, $I_{\mathrm{D}m}(t)$, and $T_{\mathrm{DIP}m}(t)$ obey linearized versions of Eqs. 30, 31, and 33 given by

$$\frac{dT_{\mathrm{DIP1}}}{dt} = kT^{\mathrm{ss}}V_{\mathrm{DIP}} - \left(d + kV^{\mathrm{ss}}\right)T_{\mathrm{DIP1}}$$

$$\frac{dI_{\mathrm{D1}}}{dt} = kV^{\mathrm{ss}}T_{\mathrm{DIP1}} - \delta I_{\mathrm{D1}} \qquad (45)$$

$$\frac{dV_{\mathrm{DIP}}}{dt} = n\delta\rho_1\psi_1 I_{\mathrm{D1}} - cV_{\mathrm{DIP}}$$

Multiply-infected cells (i.e. $I_{\mathrm{D}\ m}$ and $T_{\mathrm{DIP}\ m}$ for $m \geq 2$) do not emerge here, because they correspond to 2nd or higher-order terms in the small variable $V_{\mathrm{DIP}}$.

At large times, the three variables in Eq. 45 depend on time as $\exp(\lambda_{\max}t)$, where $\lambda_{\max}$ is the largest eigenvalue of the dynamic matrix in the right-hand side, **D**. The condition of DIP expansion is $\lambda_{\max} > 0$. Using the standard eigenvalue equation $\det[\mathbf{D}-\lambda\mathbf{1}] = 0$, together with $V^{\mathrm{ss}}$ and $T^{\mathrm{ss}}$ from Eqs. 44, and $R_0 = bkn/cd$, we obtain from standard eigenvalue analysis

$$\rho_1\psi_1 > \frac{R_0}{R_0 - 1} \qquad (46)$$

The equivalent condition was previously obtained for the model version that assumed a single copy of DIP provirus in dually infected cells [1]. This coincidence is expected, because multiple infection with DIP is negligible when DIP load is still low. (Note that the DIP load at $\eta = 1$ in Fig. 2d vanishes at the value of $\kappa$ where the condition in Eq. 46 is violated. The result is consistent with a continuous transition in DIP load from a stable DIP-free state to a stable steady state with DIP.)

*Dynamic stability of DIP at small waste parameter $\kappa << 1$*

At small waste parameter, $\kappa << 1$, using Eqs. 20 and 25-26, we predict that the state with DIP is stable if

$$\eta > \frac{1+P}{P}\frac{R_0}{R_0 - 1} \qquad (47)$$

For example, for $P = 5$ and $R_0 = 10$, the stability interval is $\eta > 1.3$. The biological meaning of condition in Eq. 47 is that for DIP to be stable, HIV must generate extra capsids for DIP to parasitize. For moderately wasteful process ($\kappa > 1$), the condition is relaxed, and $\eta$ can be a bit smaller than unity (see Fig. 2d, $\eta = 1$ curve).

## C. Evolutionary stability of DIP

*Selection coefficient of HIV in the presence of DIP at in vivo scale*

The here aim is to determine whether HIV can escape its parasite and reach the region where the population of dually infected cells becomes unstable and DIP becomes extinct. To do so, we must determine the direction of HIV evolution in the presence of DIP in parameter space. In this subsection, we focus on evolution at *in vivo* scale (i.e. individual-patient level) and use a standard approach from population genetics based on the selection coefficient and fitness. In the next subsection, we will connect fitness to the level of intracellular dynamics using the capsid-stealing model.

The fitness of a virus strain is determined by the average progeny number, i.e., the number of cells in a new generation infected by virions from a cell from the previous generation. At steady state, the average progeny number is equal to one. If an HIV mutation occurs, the mutant strain will have a smaller or larger average progeny number; the relative difference is referred to as the "selection coefficient" $s_{\text{eff}}$. Depending on the sign of $s_{\text{eff}}$, the mutant will either expand as $\exp[(s_{\text{eff}}\delta)t]$ and spread onto entire population, or go extinct. Here, $1/\delta$ is the time interval of one generation, equal to the average lifetime of an infected cell.

Note that even a beneficial mutation emerging within a genetically diverse population is likely to become extinct due to the combination of random drift and linkage effects. Indeed, a mutation must occur within a high-fitness strain to become amplified and 'fixed' in a population. Complex mathematical theories have recently been developed to describe the fixation probability and the speed of evolution in asexual models and models with rare recombination [6,7,8,9,10,11,12,13,14]. In the present work, we do not consider these complexities: our interest is in the general direction of evolution rather than its exact speed, and in the sign of $s_{\text{eff}}$ as the pointer. We assume a deterministically large population, and a single mutation with small fitness effect, as given by $|s_{\text{eff}}| << 1$.

Even this relatively simple task faces obstacles. Our system comprises virus-infected cell types $I(t)$ and $I_{Dm}(t), m = 1,2,\ldots$, with different burst sizes and different contributions to the effective selection coefficient. Our general approach to calculation of $s_{\text{eff}}$ is as follows. We start from a steady-state population, with state variables given by Eqs. 34–39. Consider a mutation in the dominant HIV strain. We note that infectivity parameter $k$ always enters any results as a product $kn$. Therefore, without any loss in generality, we will assume that only $n$ changes due to mutations. We postulate that mutation changes all burst sizes for HIV in two cell types and for IP, as given by

$$n \to n(1+\Delta_n), \psi_m \to \psi_m(1+\Delta_{\psi m}), \rho_m \to \rho_m(1+\Delta_{\rho m}), \tag{48}$$

Here increments $\Delta_n, \Delta_{\psi m}, \Delta_{\rho m}$ are considered input parameters. We then inject a small amount of the mutant virus strain, $V^{\text{mut}}(0)$. Dynamics of the mutant subpopulations $V^{\text{mut}}(t), I^{\text{mut}}(t), I^{\text{mut}}_{\text{D}\,m}(t)$ can be calculated from Eqs. 29, 31, and 32, as follows. Ahile the mutant strain is still a small fraction of a population, it weakly perturbs the rest of population, which remains near steady state (Eqs. 34–39). We introduce rescaled sizes of mutant subpopulations, $x$, $y_m$, and $z$, defined as

$$
\begin{aligned}
I^{\mathrm{mut}}(t) &= I^{\mathrm{ss}} x(t) \\
I^{\mathrm{mut}}_{\mathrm{D}\,m}(t) &= I^{\mathrm{ss}}_{\mathrm{D}\,m}\, y_m(t) \\
V^{\mathrm{mut}}(t) &= V^{\mathrm{ss}} z(t)
\end{aligned}
\tag{49}
$$

In this notation, Eqs. 29, 31, and 32 take the form

$$
\begin{aligned}
\frac{dx}{dt} &= (z - x)\delta \\
\frac{dy_m}{dt} &= (z - y_m)\delta, \quad m = 1,2,\ldots
\end{aligned}
\tag{50}
$$

$$
z + \frac{1}{c}\frac{dz}{dt} = \frac{R_0(1+\Delta_n)}{1+v+v_{DIP}}\left[ x + \sum_{i=1}^{\infty} \psi_i (1+\Delta_{\psi i}) q^i y_i \right] \tag{51}
$$

(Note that the mutational change in the DIP burst size, $\Delta_{\rho m}$, does not enter these equations.) Neglecting the time derivative on the left hand side of Eq. 51 due to the strong numerical inequality $c >> d$ (see Table S1) and substituting $R_0 / (1 + v + v_{DIP})$ from Eq. 38 into 51, the latter simplifies to

$$
z = \frac{1+\Delta_n}{1+\sum_{i=1}^{\infty} \psi_i q^i}\left[ x + \sum_{i=1}^{\infty} \psi_i (1+\Delta_{\psi i}) q^i y_i \right] \tag{52}
$$

The asymptotic expressions for variables $x(t)$, $y_m(t)$, and $z(t)$ at large times $t$ have the exponential form $\exp[(s_{\mathrm{eff}}\delta)t]$, so that Eqs. 50 reduce to

$$
z = (1+s_{\mathrm{eff}})x = (1+s_{\mathrm{eff}})y_m \tag{53}
$$

Substituting Eq. 53 into 52 and neglecting second-order terms in $\Delta$, we obtain

$$
s_{\mathrm{eff}} = \Delta_n + \frac{\sum_{i=1}^{\infty} \psi_i q^i \Delta_{\psi i}}{1+\sum_{i=1}^{\infty} \psi_i q^i} \tag{54}
$$

where $\psi_i$ is given by Eqs, 14, 18, 19 (for $\kappa = 0$, by simplified Eqs. 25 to 27), and $q$ is found from solving Eqs. 38, 39, and 42 (result in Fig. S3a).

Thus, the selection coefficient $s_{\mathrm{eff}}$ has contributions from two relative changes caused by mutation: in the base burst size, $n$, and in the HIV suppression factor due to the presence of $i$ copies of DIP, $\psi_i$.

*Specific expression for the selection coefficient in the intracellular model*

In the previous subsection, we expressed the effective selection coefficient of mutation in the HIV genome, in the general form, in terms of relative changes in burst sizes $n$, $n\psi_{\mathrm{m}}$, and $n\rho_m\psi_m$ due to mutation. Now, we will express it in terms of parameters of the single-cell model. The burst sizes are determined by $\eta, \kappa$, $P$, $m$, and $\theta/\delta$ (Eqs. 14, and 18–20). The expression asymmetry, $P$, is fixed by the molecular architecture of the DIP and $m$ is the index in a sum. It is also obvious that HIV evolves towards larger capsid numbers $\eta$ (see two subsections down) and $\theta/\delta$, but there is a natural limit to such an increase, and it does not reflect on DIP stability since $\eta$ increases all burst sizes equally (both the HIV burst from dually and singly infected cells and the DIP burst from dually infected cells). Therefore, we focus on evolution in the remaining parameter, the waste parameter $\kappa$ (defined by Eq. 13). $\kappa$ can evolve, for example, by changing packaging parameter $k_{\mathrm{pck}}$, which is controlled by the amino-acid sequence in HIV *gag* and the corresponding RNA sequence in the HIV SL3 loop. Since *gag* and SL3 mutations would reduce DIP stealing but also reduce HIV burst size, the direction of evolution in $\kappa$ is not obvious.

*Calculations for Fig 3: Effect of mutation in the waste parameter*

We denote mutational change in parameter $\kappa$ as $\partial\kappa_{\mathrm{mut}}$. Mutations that relax packaging result in increased $\kappa$, $\partial\kappa_{\mathrm{mut}} > 0$. In singly infected cells ($I$), such a mutation is deleterious to HIV because it decreases the burst size. However, singly infected cells are rare, and their fraction is on the order of $1/E[m] \sim 1\text{-}q$ (Eq. 37), where $1\text{-}q$ is small (Fig. S3a). In the dominant population of dually infected cells ($I_{\mathrm{D}m}$), the same mutation may be favorable, because reduction in packaging also reduces capsid stealing by DIP. Formally, the two terms in the numerator of Eq. 54 should have different signs. Below, we confirm this intuitive prediction and show that both effects are of the same order, but the first effect (deleterious reduction in HIV burst size) wins and results in selection against increases in $\kappa$.

From Eqs. 18–19, for the relative changes in the HIV burst size in singly and dually infected cells ($n$ and $n\psi_m$, respectively), we obtain

$$\Delta_n = \partial\kappa_{\mathrm{mut}} \frac{\partial}{\partial\kappa} \ln\left[\frac{y}{1+y}\right]_{P=0}$$
$$\Delta_n + \Delta_{\psi m} = \partial\kappa_{\mathrm{mut}} \frac{\partial}{\partial\kappa} \ln\frac{y}{1+y} \qquad (55)$$

respectively, where $y$ as a function of $\kappa$ is given by Eq. 14. Substituting $\Delta_n$ and $\Delta_{\psi m}$ from Eqs. 55 into 54 and computing $q$ numerically from Eqs. 38, 39, and 42, we calculate the desired value of $s_{\mathrm{eff}}$.

The results are shown in Fig. 3. As expected, the factor of HIV suppression by DIP favors mutations increasing waste parameter $\kappa$. However, the overall decrease in the HIV burst size dominates evolution: HIV evolves towards smaller waste parameters. We conclude that HIV cannot shake off DIP by bringing it to the threshold of extinction.

We assumed equal packaging constants for DIP and HIV. Once equal, they will remain evolutionary stable. Indeed, a mutation in HIV *gag* (used by both HIV and DIP) decreases the two constants equally. In principle, a second compensatory mutation in HIV SL3 loop could partly restore packaging for HIV while leaving DIP packaged inefficiently. However, an

identical mutation in SL3 loop of DIP will immediately restore high packaging efficiency of DIP. Compensation in DIP will occur rapidly, because it occurs in a larger population (DIP provirus population is larger than HIV provirus population) and is a single mutation rather than a pair of corresponding mutations in Gag structure and SL3 needed for HIV to switch to an alternate efficient packaging scheme. The rate of single mutation in DIP can be estimated to be higher by a factor of $V_{\mathrm{DIP}} s_{\mathrm{eff}}/V\mu$. Thus, unlike in the case of the genome-stealing mechanism (main text), compensatory mutation in HIV does not cause divergent evolution of HIV and DIP.

Effect of mutation in the capsid-to-genome production ratio $\eta$

In the same way, we can predict the effective selection coefficient for mutations increasing the capsid-to-genome production ratio $\eta$ by $\partial\eta_{\mathrm{mut}}$. Replacing the derivatives in $\kappa$ with derivatives in $\eta$ in Eq. 55, leads to the following forms for relative changes in burst sizes of HIV in singly and dually infected cells, respectively:

$$\Delta_n = \partial\eta_{\mathrm{mut}} \frac{\partial}{\partial\eta} \ln\left[\frac{y}{1+y}\right]_{P=0}$$

$$\Delta_n + \Delta_{\psi m} = \partial\eta_{\mathrm{mut}} \frac{\partial}{\eta} \ln\frac{y}{1+y}$$

where $y$ is determined by Eq. 14.

As we have shown in the previous subsection, HIV evolves toward smaller waste parameters, $\kappa << 1$. In the limit of small $\kappa$, it is more convenient to use directly Eqs. 23 and 25-27 for the burst size $n$ and the suppression factor $\psi_m$, to find

$$\Delta_n = \begin{cases} \partial\eta_{\mathrm{mut}}/\eta, & \eta < 1 \\ 0, & \eta > 1 \end{cases} \tag{56}$$

and

$$\Delta_{\psi m} = \begin{cases} 0, & \eta < 1 \\ \partial\eta_{\mathrm{mut}}/\eta & 1 < \eta < 1 + mP \\ 0, & \eta > 1 + mP \end{cases} \tag{57}$$

The selection coefficient $s_{\mathrm{eff}}$ is derived by substituting the relative changes, Eqs. 56 and 57, into Eq. 54, In Eq. 54, we use Eqs. 25 to 27 for suppression factor $\psi_{\mathrm{i}}$. and numeric solution of Eqs. 38,39, and 42 for $q$.

Here we assume that DIP is dynamically stable in an individual host, which is true under the condition $\eta > \eta_{\mathrm{c}} = (P+1)R_0/[P(R_0-1)]$ where $\eta_{\mathrm{c}}$ is slightly larger than 1 (Eq. 47). To take DIP stability into account, the interval boundary between the first and second interval in Eq. 57 is slightly shifted from to $\eta=1$ to $\eta=\eta_{\mathrm{c}}$

The final result for selection coefficient of mutation in $\eta$ is shown in Fig. 4. As expected, HIV favors increase in capsid production in the entire range of $\eta$. Indeed, both terms in Eq. 54 are non-negative, and we have positive selection coefficient $s_{\text{eff}} > 0$. The magnitude of the selection coefficient, however, depends on $\eta$ and the presence of IP. At $\eta < 1$, when DIP is absent, HIV strongly favors increases in $\eta$ due to increases in its burst size (first term in Eq. 54; 2nd term is zero). At $\eta_c < \eta < P+1$, increases in capsid production is also strongly preferred, due to the presence of DIP, which steals most capsids in dually infected cells (second term in Eq. 54; first term in Eq. 54 is zero).

Interestingly, in a narrow interval of $\eta$, such that $1 < \eta < \eta_c$, selection coefficient is zero (in Eq. 54, $\Delta_n = q = 0$). Intuitively, HIV already has more capsids than it needs to package its genomes (i.e. $\eta > 1$) and DIP suppression is absent. Only a finite rate of product loss (i.e. finite $\kappa$) weakly favors production of extra capsids and results in small, positive selection coefficient (in Eq. 54, $q = 0, \Delta_n > 0$).

Suppose, an HIV strain with $\eta < 1$ infects a person in a population infected with an older strain of HIV with DIP present. During evolution within the person, the value of $\eta$ in the new strain will evolve rapidly to $\eta = 1$; then, its increase will slow down significantly. When the DIP stability threshold $\eta = \eta_c$ is reached, DIP can enter by co-infecting the person from an outside population. Further increases in $\eta$ will accelerate again until the biological ceiling (due to mRNA degradation) is reached. This raises interesting questions regarding competition in human populations between two HIV strains with a high and a low upper limit on capsid production (the main text, *Discussion*).

## D. Estimate of intracellular model parameters $\kappa$ and $\eta$ for HIV in vivo

So far, our consideration was general. It is instructive to place parameters within the context of HIV infection *in vivo*. In Figs. 2–3 the results depend on four parameters $R_0$, $P$, $\eta$, and $\kappa$. $R_0$ is set in patients (with an average of $R_0$~10) and $P$ is set by the molecular design of the DIP, which leaves the parameters $\eta$ and $\kappa$. Direct estimates of these two parameters may be difficult, because they describe the rate of processes consisting of many consecutive stages. Below, we estimate them indirectly, relating $\eta$ and $\kappa$ to two dynamic quantities, the successful fractions of genomes and capsids, $f_G$ and $f_C$, respectively. By definition, successful genomes are those that do not decay but are packaged within released virions. "Successful" capsids are released with a dimerized HIV genome inside, rather than a single RNA copy, no RNA (i.e. empty) or with irrelevant non-gRNAs. From *in vivo* data in the literature, we can estimate $f_C$ and obtain a relation between $\eta$ and $\kappa$.

We consider cells infected with HIV only. Steady-state conditions for Eqs. 1 and 2 have the form

$$\begin{aligned} \theta &= k_{\text{pck}} GC + \alpha G \\ \eta\theta &= k_{\text{pck}} GC + \beta C \end{aligned} \tag{58}$$

By definition, fractions of "successful" capsids and genomes are given by

$$f_C = \frac{k_{pck} GC}{\eta\theta}, \quad f_G = \frac{k_{pck} GC}{\theta} \tag{59}$$

which yields

$$\eta = f_G / f_C \tag{60}$$

Definition of parameter $\kappa$ in Eq. 13 can be written as

$$\kappa = \frac{\alpha G}{\theta} \frac{\beta C}{k_{\text{pck}} GC} = (1 - f_G) \frac{(1 - f_C)}{f_C} \tag{61}$$

where we used Eqs. 56–57. Excluding $f_G$ from Eqs. 60 and 61, we obtain a linear relationship between $\eta$ and $\kappa$

$$\eta + \frac{\kappa}{1 - f_C} = \frac{1}{f_C} \tag{62}$$

In principle, the fraction of non-empty released capsids $f_C$ is measurable and has been estimated previously as $f_C \sim 0.2$ (Ref. [15], Appendix D). The estimate compared two measurements of the average viremia peaks measured in MAMU A*01 rhesus macaques infected with SIVmac251: one by p24 Ab assay [16] and another by sensitive branching DNA assay [17,18]. A recent *in vitro* study, using a two-RNA labeling technique, predicted a much higher value, $f_C > 0.9$, for an engineered HIV strain infecting a cell line [19]. However, due to assay fidelity, the reliability of these estimates of $f_c$ *in vivo* must be taken with a degree of caution.

The relationship between $\eta$ and $\kappa$ given by Eq. 60 and the region of dynamic instability of DIP is shown in Fig. S4. Thus, the larger $\eta$ the smaller $\kappa$, and both do not exceed $1/f_C \sim 5$ (or larger). Because HIV tends to evolve towards small $\kappa$ and large $\eta$ (Fig. 3 and sections above), it is reasonable to conjecture that $\eta$ is close to $1/f_C$ and far from the instability region of DIP. Studies

in vitro in broader range of cell types could verify the value of $f_C$ and the inferred capsid-to-genome ratio.

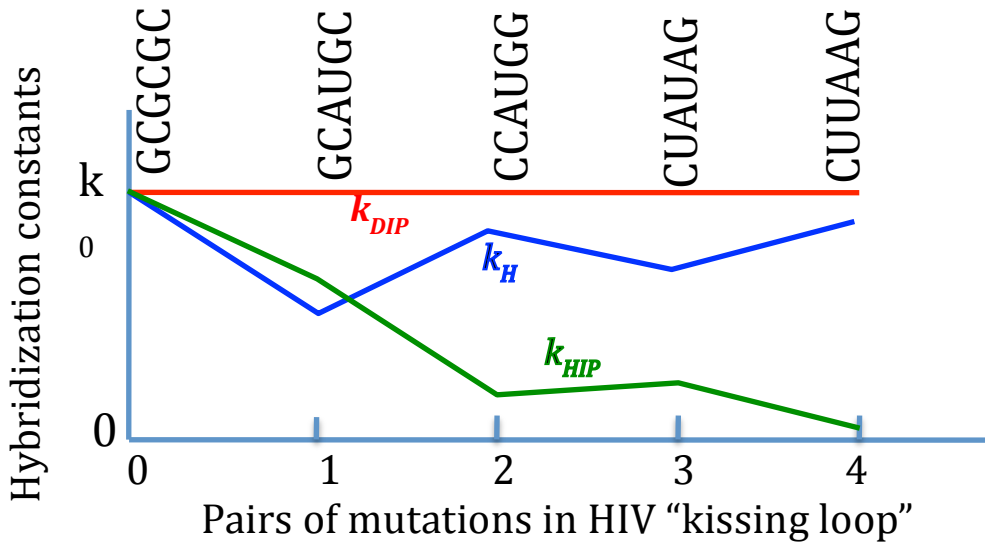


**Figure S1: Evolution in the dimerization initiation sequence leads to sequence divergence between HIV and DIP.** An example of an evolving palindromic SL1 sequence is shown on the top. Initial sequence is the same for DIP and HIV, GCGCGC, IP sequence remains unchanged. Dimerization coefficients for HIV-HIV, HIV-DIP and DIP-DIP (defined in Equations in Fig. 1b) are shown qualitatively versus mutation pair number. Each pair includes a mutation in the 6-residue SL1 loop causing a palindrome mismatch, and a compensatory mutation, which restores palindrome. Each dimerization constant $k_H$, $k_{IP}$, $k_{HIP}$, has an idealized component determined by the number of mismatches (see Fig. 1c-d for details), and a fluctuating component, which depends on specific palindrome sequence (and SL1 stem sequence as well). HIV-DIP cross-dimerization coefficient decreases as the loop sequence diverges from GCGCGC, while HIV-HIV dimerization coefficient fluctuates around a constant level.

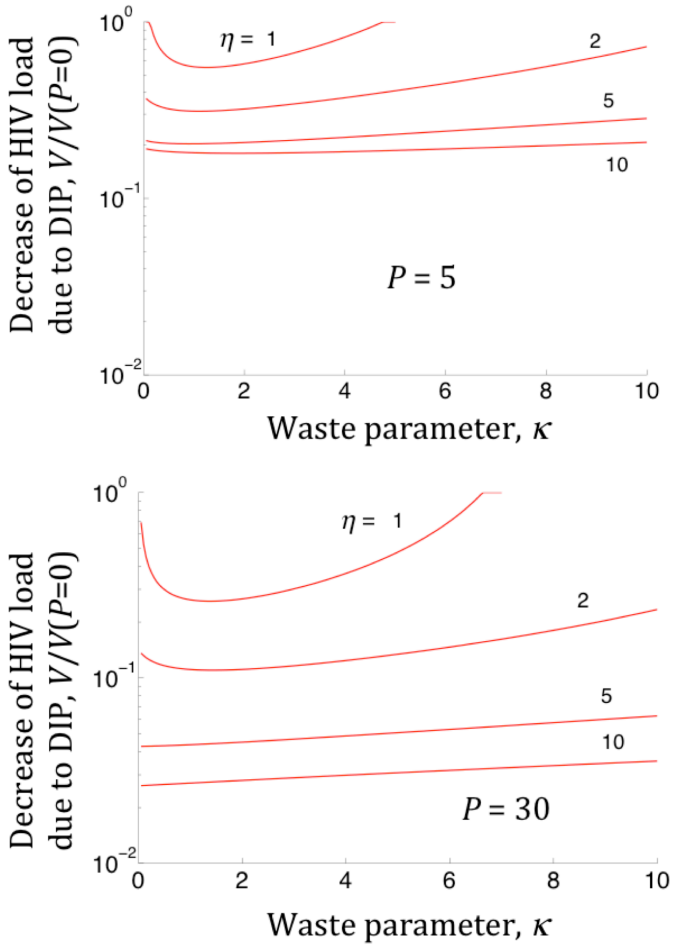


**Figure S2: DIP contribution to suppression of HIV-1 viral load.** The curves show the ratio of HIV load to its value in the absence of DIP ($P = 0$). Values of $\eta$ and $P$ are shown. When both $P$ and $\eta$ are sufficiently large, > 5, the main decrease in HIV load at finite $\kappa$ is due to suppression by DIP rather than to the loss of HIV products (compare to Fig. 2b).

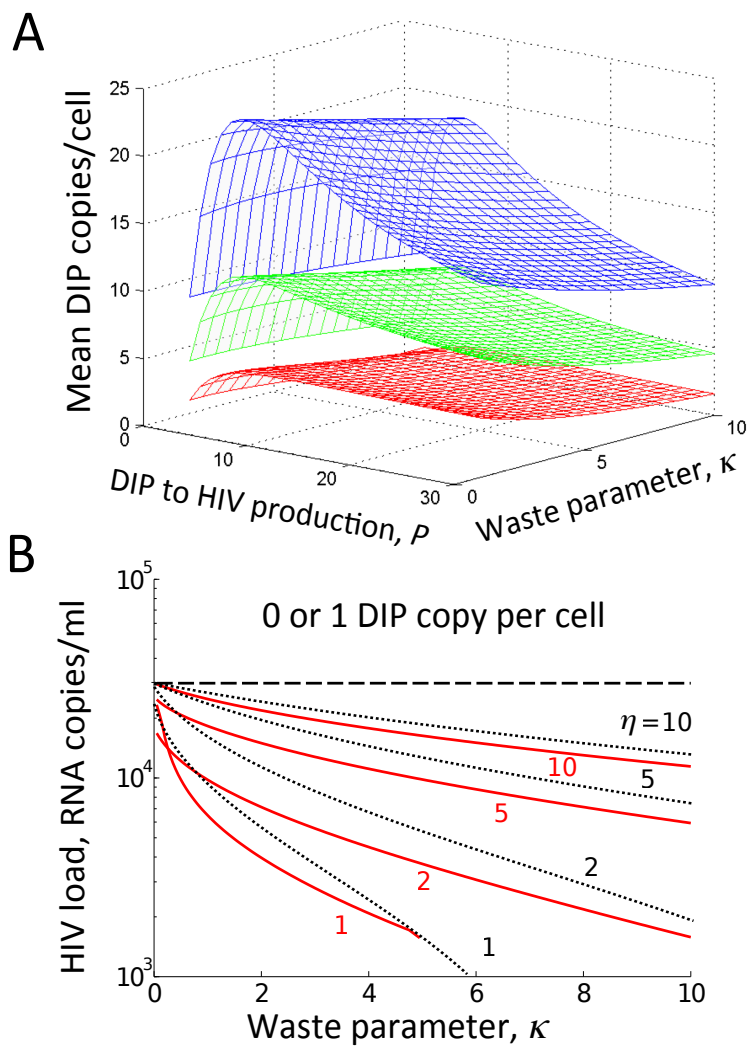


**Figure S3**. **The average multiplicity of DIP infection is high, which enhances suppression of HIV-1**. *(a)* Average number of DIP provirus copies per cell $E[m] = 1/(1-q)$ is shown as a function of waste parameter $\kappa$, at several values of $\eta$: $\eta = 2$ (red), $\eta = 5$ (green), $\eta = 10$ (blue). Values in the vertical axis are calculated as $1/(1-q)$, where $q$ is the ratio of the cell number with $m$+1 copies to the cell number with $m$ copies, (see *Methods in SI Text*). Unity at the vertical axis corresponds to a DIP-free population. The DIP subpopulation is unstable at small and large $\kappa$ when $\eta \sim 1$, and at large $\kappa$ when $\eta > 1.7$. Multiple copies of DIP provirus per cell amplify DIP genomic mRNA amount in cells and at the level of the individual, and amplify suppression of HIV-1 load. *(b)* Steady-state HIV-1 load when multiplicity of DIP infection, $m$, is restricted to $\leq 1$. HIV-1 suppression is markedly decreased at larger $\eta$ (cf. Fig. 2a) since a single copy of DIP provides much weaker interference; at $m \leq 1$ suppression of HIV-1 is primarily due to the loss of HIV-1 products at large $\kappa$ (cf. Fig. 2b). Parameters used are as described in main text Fig. 2 (i.e. $R_0 = 10$, $P = 5$).

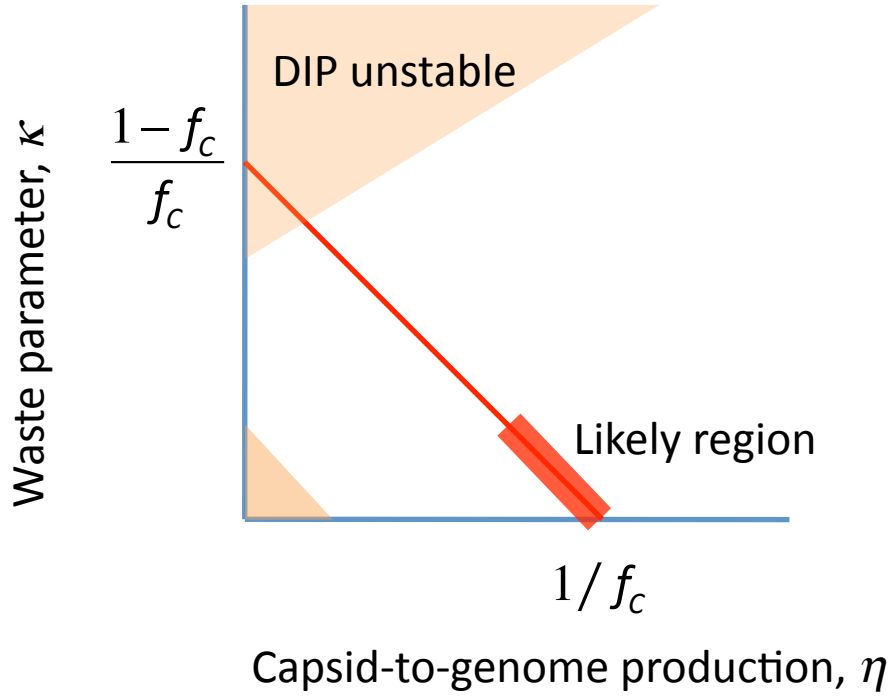


1 3

2 **Figure S4: In vivo estimates for waste parameter $\kappa$ and capsid-to-genome production $\eta$ are**
3 **inversely related.** The fraction of non-empty virions is $f_C \sim 0.2$ for HIV, according to [15,20].
4 The likely region of actual parameters (thick red line) is far from regions of DIP instability
5 (orange shade, compare with Fig. 2d).

6
7

## Supporting References


1. Metzger VT, Lloyd-Smith JO, Weinberger LS (2011) Autonomous targeting of infectious superspreaders using engineered transmissible therapies. PLoS computational biology 7: e1002015.

2. Weinberger LS, Schaffer DV, Arkin AP (2003) Theoretical design of a gene therapy to prevent AIDS but not human immunodeficiency virus type 1 infection. J Virol 77: 10028-10036.

3. Perelson AS, Nelson PW (1999) Mathematical analysis of HIV-1 dynamics in vivo. Siam Review 41: 3-44.

4. Nowak MA, May RM (2000) Virus dynamics : mathematical principles of immunology and virology. Oxford ; New York: Oxford University Press. xii, 237 p. p.

5. Josefsson L, King MS, Makitalo B, Brannstrom J, Shao W, et al. (2011) Majority of CD4+ T cells from peripheral blood of HIV-1-infected individuals contain only one HIV DNA molecule. Proc Natl Acad Sci U S A 108: 11199-11204.

6. Tsimring LS, Levine H, Kessler D (1996) RNA virus evolution via a fitness-space model. Phys Rev Lett 76: 4440-4443.

7. Rouzine I, Wakeley J, Coffin J (2003) The solitary wave of asexual evolution. Proc Natl Acad Sci U S A 100: 587-592.

8. Rouzine IM, Brunet E, Wilke CO (2008) The traveling-wave approach to asexual evolution: Muller's ratchet and speed of adaptation. Theor Popul Biol 73: 24-46.

9. Desai MM, Fisher DS (2007) Beneficial mutation selection balance and the effect of linkage on positive selection. Genetics 176: 1759-1798.

10. Rouzine IM, Coffin JM (2005) Evolution of human immunodeficiency virus under selection and weak recombination. Genetics 170: 7-18.

11. Rouzine IM, Coffin JM (2007) Highly fit ancestors of a partly sexual haploid population. Theor Popul Biol 71: 239-250.

12. Rouzine IM, Coffin JM (2010) Multi-site adaptation in the presence of infrequent recombination. Theor Popul Biol 77: 189-204.

13. Hallatschek O (2010) The noisy edge of traveling waves. Proc Natl Acad Sci U S A 108: 1783-1787.

14. Neher RA, Shraiman BI, Fisher DS (2010) Rate of adaptation in large sexual populations. Genetics 184: 467-481.

15. Sergeev RA, Batorsky RE, Rouzine IM (2010) Model with two types of CTL regulation and experiments on CTL dynamics. J Theor Biol 263: 369-384.

16. Kuroda MJ, Schmitz JE, Charini WA, Nickerson CE, Lifton MA, et al. (1999) Emergence of CTL coincides with clearance of virus during primary simian immunodeficiency virus infection in rhesus monkeys. J Immunol 162: 5127-5133.

17. Letvin NL, Mascola JR, Sun Y, Gorgone DA, Buzby AP, et al. (2006) Preserved CD4+ central memory T cells and survival in vaccinated SIV-challenged monkeys. Science 312: 1530-1533.

18. Sun Y, Schmitz JE, Buzby AP, Barker BR, Rao SS, et al. (2006) Virus-specific cellular immune correlates of survival in vaccinated monkeys after simian immunodeficiency virus challenge. J Virol 80: 10950-10956.

19. Chen J, Nikolaitchik O, Singh J, Wright A, Bencsics CE, et al. (2009) High efficiency of HIV-1 genomic RNA packaging and heterozygote formation revealed by single virion analysis. Proc Natl Acad Sci U S A 106: 13535-13540.

20. Sergeev RA, Batorsky RE, Coffin JM, Rouzine IM (2010) Interpreting the effect of vaccination on steady state infection in animals challenged with Simian immunodeficiency virus. J Theor Biol 263: 385-392.